

# CONTENTS

CHINESE ABSTRACT .....	I
ABSTRACT .....	III
ACKNOWLEDGEMENTS .....	V
CONTENTS .....	VI
LIST OF FIGURE CAPTIONS .....	IX
LIST OF TABLE CAPTIONS .....	XIV
1. INTRODUCTION.....	1
1.1 Motivation.....	1
1.2 Literature Survey.....	1
1.3 Contributions of the Dissertation.....	5
1.4 Outline of the Contents.....	8
2. DERIVATION OF EQUIVALENT DC BRUSH MOTOR MODEL OF THE PMBLDCM FOR SYSTEM INTEGRATION .....	10
2.1 Introduction .....	10
2.2 Review of the Conventional Mathematic Models.....	10
2.3 Derivation of the Proposed Equivalent DC Brush Motor Model....	16
3. TRI-MODE CONTROL AND SYNTHESIS OF THE EQUIVALENT ARMATURE CURRENT FOR REDUCING TORQUE RIPPLES.....	22
3.1 Introduction.....	22
3.2 Sensing of the Complete Three-Phase Currents of PMBLDC	

Motors .....	23
3.3 The Proposed Tri-Mode Control of the Equivalent Armature Current.....	28
3.4 Synthesis of the Equivalent Armature Current of PMBLDC Motors .....	36
3.5 Simulation Results of the Proposed Tri-Mode Equivalent Armature Current Controlled PMBLDC Motor System.....	37
4. THE PROPOSED PLL ASSISTED ADJUSTABLE SPEED CONTROL STRATEGY .....	49
4.1 Introduction .....	49
4.2 The Proposed PLL Assisted Speed Control Strategy .....	50
4.3 Derivation of Closed Form Expressions of $k_p$ and $k_I$ Parameters of the PI Controller .....	54
4.4 Stability Analysis of the Closed-Loop System .....	57
5. IMPLEMENTATION AND EXPERIMENTAL RESULTS .....	64
5.1 Introduction.....	64
5.2 Description of the Test Drive System .....	65
5.3 Implementation of the Proposed Drive System.....	70
5.4 Simulation and Experimental Results.....	85
6. CONCLUSIONS .....	96
REFERENCES.....	100

APPENDIX A	THE EQUIVALENT DC BRUSH MOTOR MODEL OF THE INTERIOR PMBLDC MOTOR .....	106
APPENDIX B	THE PMBLDC MOTOR .....	112



## LIST OF FIGURE CAPTIONS

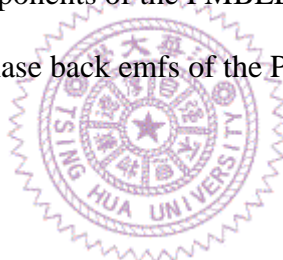
Fig. 1.1	Circuit diagram of the linear current sensing IC, IR2175, for the motor phase current sensing .....	3
Fig. 1.2	The dc-link current sensing method for the motor phase current sensing .....	4
Fig. 2.1	Schematic diagram of an elementary two-poles dc machine.....	11
Fig. 2.2	Schematic diagram of a typical PMBLDC motor with a full-bridge inverter. .	13
Fig. 2.3	Typical waveforms of the emfs, phase currents and the corresponding gating signals for the PMBLDC motor drives.....	14
Fig. 2.4	Typical waveforms of the emfs, phase currents and the proposed commutation functions for the PMBLDC motor drives .....	17
Fig. 2.5	The proposed equivalent dc brush motor model for the PMBLDC motors.....	20
Fig. 3.1	Notations defined for the PMBLDC motor drive .....	23
Fig. 3.2	Steady state ideal waveforms of the back emfs, phase currents and the corresponding gating signals.....	24
Fig. 3.3	Current flow diagrams under three control modes for interval I. (a) active mode. (b) freewheeling mode. (c) regenerative mode.....	26
Fig. 3.4	Schematic diagram of the PWM control under driving and braking conditions. ....	27
Fig. 3.5	The proposed current sensing scheme under three control modes for interval I. (a) active mode. (b) freewheeling mode. (c) regenerative mode.....	29
Fig. 3.6	Hall sensor signals of the PMBLDC motor. ....	30
Fig. 3.7	The block diagram of the integrated phase current sensing and equivalent armature current control system .....	32

Fig. 3.8	The block diagram of the integrated phase current sensing and equivalent armature current synthesise and control system.....	33
Fig. 3.9	Complete operation modes for the proposed equivalent armature current sensing and synthesis method cases I(a), I(b) and I(c) in interval I. ....	38
Fig. 3.10	Complete operation modes for the proposed equivalent armature current sensing and synthesis method cases II(a), II(b) and II(c) in interval II.....	39
Fig. 3.11	Complete operation modes for the proposed equivalent armature current sensing and synthesis method cases III(a), III(b) and III(c) in interval III.....	40
Fig. 3.12	Complete operation modes for the proposed equivalent armature current sensing and synthesis method cases IV(a), IV(b) and IV(c) in interval IV.. ....	41
Fig. 3.13	Complete operation modes for the proposed equivalent armature current sensing and synthesis method cases V(a), V(b) and V(c) in interval V.....	42
Fig. 3.14	Complete operation modes for the proposed equivalent armature current sensing and synthesis method cases VI(a), VI(b) and VI(c) in interval VI.....	43
Fig. 3.15	Transient simulation results of $i_b$ , $i_c$ , $i_{eq}$ and $T_e$ with the proposed equivalent armature current control under commutation process assuming ideal trapezoidal back emfs. ....	45
Fig. 3.16	Transient simulation results of $i_b$ , $i_c$ , $i_{eq}$ and $T_e$ without the proposed equivalent armature current control under commutation process assuming ideal trapezoidal back emfs. ....	46
Fig. 3.17	Trapezoidal back emfs with spreading angle around 100°. ....	46
Fig. 3.18	Transient simulation results of $i_b$ , $i_c$ , $i_{eq}$ and $T_e$ without the proposed equivalent armature current control under commutation process assuming non-ideal trapezoidal back emfs. ....	47

Fig. 3.19	Transient simulation results of $i_b$ , $i_c$ , $i_{eq}$ and $T_e$ with the proposed equivalent armature current control under commutation process assuming non-ideal trapezoidal back emfs.....	47
Fig. 4.1	The proposed PLL assisted speed controller of the PMBLDC drive.....	50
Fig. 4.2	The relationship between the Hall-sensor signals, $h_a$ , $h_b$ , $h_c$ , the pulse signals, $f_a$ , $f_b$ , $f_c$ and the motor speed pulse train signal $f_r$ .....	51
Fig. 4.3	State transition diagram of the PFD.....	53
Fig. 4.4	The typical internal reference model control structure for the PMBLDC motor .....	54
Fig. 4.5	The classic control structure for the PMBLDC motor .....	55
Fig. 4.6	Speed response simulations of the proposed system for different time constant $T_p$ . (a) $T_p=0.2\text{sec}$ . (b) $T_p=0.3\text{sec}$ . (c) $T_p=0.1\text{sec}$ .....	57
Fig. 4.7	(a) Average output voltage of 4046 PFD with the input of frequency difference between $f_s$ and $f_r$ under unlocked condition. (b) Output curve of PFD with the $\cos\theta$ input under unlocked condition. ....	58
Fig. 4.8	The proposed PLL assisted speed controller of the PMBLDC with describing function $D(\omega_{er})$ .....	60
Fig. 4.9	Stability margin for the variation of system parameters $k$ and $T_f$ of the proposed controller. ....	62
Fig. 5.1	Configuration of the test system .....	65
Fig. 5.2	The schematic diagram of the proposed drive. (a) current controller. (b) speed controller.....	67
Fig. 5.3	The completed prototype system (a) With a magnetic powder clutch test load. (b) With an industrial blower test load.....	69

Fig. 5.4	The hardware implementation circuits of the power circuits .....	71
Fig. 5.5	The dc power supply circuit for control circuits.....	73
Fig. 5.6	The graphic editorial circuit of the CPLD chip EPM7064 output from ALTERA MAX+plus II developing software. ....	75
Fig. 5.7	The hardware implementation circuits of Block B in Fig. 5.2(a).....	78
Fig. 5.8	The hardware implementation circuits of Block C in Fig. 5.2(a).....	80
Fig. 5.9	The hardware implementation circuits of Blocks A and D in Fig. 5.2(a).....	81
Fig. 5.10	The hardware implementation circuits of the PLL control loop of the proposed speed controller .....	83
Fig. 5.11	The hardware implementation circuits of the PI control loop of the proposed speed controller .....	84
Fig. 5.12	Bode diagram of the loop gain function of the proposed controller. ....	87
Fig. 5.13	Experimental results of the motor phase current and the equivalent armature current with equivalent armature current control. (a) At 200rpm. (b) Expanded curve of Fig. 5.13(a). (c) At 800rpm. (d) Expanded curve of Fig. 5.13(c).....	88
Fig. 5.14	Experimental results of the motor phase current and the equivalent armature current without equivalent armature current control .....	90
Fig. 5.15	Waveforms of $f_s$ , $f_r$ and $\theta_{ep}$ of the proposed drive while the motor is operated at 333rpm and with different load conditions. (a) No load. (b) 5Nt-m load. (c) 9Nt-m load. ....	92
Fig. 5.16	Transient experimental results of the proposed drive. (a) Waveforms of the $\alpha$ -phase current, $\omega_r$ and $f_r$ . (b) The corresponding amplified portion of part of (a) .....	94

Fig. 5.17	Comparison of the three-phase induction motor and the self-designed PMBLDC motor of the industrial blower. (a) Comparison of the power consumption. (b) Comparison of the volume .....	95
Fig. A.1	The proposed equivalent dc brush motor model for the IPMBLDC motors ..	111
Fig. A.2	The proposed equivalent dc brush motor model for the SMPMBLDC motors .....	111
Fig. B.1	2D geometry of the self-designed PMBLDC motor.....	114
Fig. B.2	The picture of the NdFeB magnet of the PMBLDC motor .....	114
Fig. B.3	Three-phase winding diagram of the stator of the PMBLDC motor.. .....	115
Fig. B.4	The flux distribution of the PMBLDC motor with stator circuit being opened .....	115
Fig. B.5	The picture of the components of the PMBLDC motor .....	116
Fig. B.6	The measured three-phase back emfs of the PMBLDC motor. ....	116





## LIST OF TABLE CAPTIONS

Table 3.1	The proposed phase current sensing scheme .....	34
Table 3.2	Interval locating from $h_a$ , $h_b$ , $h_c$ and the corresponding steady-state switch status .....	34
Table 3.3	Coding table of the gating signal generator .....	35
Table 3.4	Coding table of the gating signals $Mx'$ , $My'$ and $Mz'$ .....	36
Table 5.1	Input/output signal relation of the Coding-Table in the CPLD chip.....	76
Table B.1	Geometric parameters of the self-designed PMBLDC motor .....	113

